Collective Quantum Memory Activated by a Driven Central Spin

Denning, Emil Vosmar; Gangloff, Dorian A.; Atatüre, Mete; Mørk, Jesper; Le Gall, Claire

Published in:
Physical Review Letters

Link to article, DOI:
10.1103/physrevlett.123.140502

Publication date:
2019

Document Version
Publisher's PDF, also known as Version of record

Collective quantum memory activated by a driven central spin

Emil V. Denning,[1,2] Dorian A. Gangloff,[2] Mete Atatüre,[2] Jesper Mørk,[1] and Claire Le Gall[2,*]

[1]*Department of Photonics Engineering, Technical University of Denmark, 2800 Kgs. Lyngby, Denmark*
[2]*Cavendish Laboratory, University of Cambridge, JJ Thomson Avenue, Cambridge CB3 0HE, United Kingdom*

(Dated: November 15, 2019)

Coupling a qubit coherently to an ensemble is the basis for collective quantum memories. A single driven electron in a quantum dot can deterministically excite low-energy collective modes of a nuclear spin ensemble in the presence of lattice strain. We propose to gate a quantum state transfer between this central electron and these low-energy excitations – spin waves – in the presence of a strong magnetic field, where the nuclear coherence time is long. We develop a microscopic theory capable of calculating the exact time evolution of the strained electron-nuclear system. With this, we evaluate the operation of quantum state storage and show that fidelities up to 90% can be reached with a modest nuclear polarisation of only 50%. These findings demonstrate that strain-enabled nuclear spin waves are a highly suitable candidate for quantum memory.

Introduction — Quantum memory working in conjunction with a computational qubit is a central element in fault-tolerant quantum computing and communication strategies [1, 2]. Prominent examples of quantum memory implementations include collective states of atomic ensembles [3–6] and rare-earth-ion doped crystals [7, 8] able to store a photonic qubit, cold ions, where the decoherence-free subspace of a local ion pair acts as memory for a single ion qubit [9, 10] and nitrogen vacancy centres in diamond, where the electronic spin state can be written into a single proximal nuclear spin [11–13]. For semiconductor quantum dots, the mesoscopic spin environment comprising $\sim 10^4 - 10^5$ nuclei is a candidate for a collective quantum memory that can store the electronic spin state [14–16], with the promise of coherence times reaching milliseconds [17]. A strategy for electron–nuclear state transfer is based on flip-flops generated by the collinear hyperfine interaction [14]. A consequence of this interaction scheme brings about opposing requirements: Vanishing electron spin splitting during the state transfer versus large electron spin splitting to polarise and stabilise the nuclear coherence [18]. An alternative approach is to use collective nuclear spin wave excitations that have recently been observed under a strong magnetic field in the form of a coherently distributed single nuclear spin excitation [19] through an effective non-collinear hyperfine interaction [20]. In this Letter, we propose a protocol for quantum memory based on this interaction, which in equilibrium is suppressed by a strong static magnetic field, but can be controllably switched on for a finite time by driving the qubit out of equilibrium.

The non-collinear hyperfine interaction responsible for qubit-controlled spin wave excitation originates from strain. In a strained lattice (cf. Fig. 1a), the induced electric field gradient couples to the quadrupole moment of the nuclei, thereby tilting the nuclear spin quantisation axis away from that dictated by the magnetic field (defining the z-axis). This strain-induced mixing of the Zeeman eigenstates allows otherwise forbidden nuclear transitions that can be accessed by the electron through the hyperfine interaction, $H_{\rm hf} = \sum_j 2A^j I_z^j S_z$ (S_z and I_z^j are electronic and jth nuclear spin-z operators). The transitions are activated when the electron spin is driven – magnetically or optically – to bridge the excitation energy gap corresponding to the nuclear Zeeman energy, $\omega_{\rm Z}^{\rm n}$.

Equipped with an interaction mechanism that can be switched on and off, information can be controllably transferred from the electron to the nuclei by letting the two subsystems interact for a finite duration. This can be realised in multiple ways; for the current proposal, we consider a Hamiltonian engineering approach based electron spin rotations on the Bloch sphere with a sequence of fast pulses [21], which selectively enhances the collective electron–nuclear transitions and simultaneously cancels out slow noise from the nuclear Overhauser field. The electron spin rotations in the pulse sequence can be carried out using an all-optical Raman drive to obtain phase-controlled manipulation at Rabi frequencies far exceeding the nuclear Zeeman splitting and hyperfine fluctuations of the electron Zeeman energy [22]. The nuclear coherence time can be extended up to milliseconds by removing the electron from the quantum dot [18] or alternatively by decoupling of the Knight field through a simple electron spin echo sequence [23, 24]. Read-out of the nuclear memory is effectuated by once again driving the electron to turn on the interaction.

Electron–nuclear exchange mechanism — The Hamiltonian describing the quadrupolar coupling of the N nuclear spins ($I > 1/2$) is

$$H_{\rm Q} = \sum_{j=1}^{N} B_{\rm Q}[(I_x^j)^2 \sin^2\theta + \frac{1}{2}(I_x^j I_z^j + I_z^j I_x^j)\sin 2\theta + (I_z^j)^2\cos^2\theta],$$

where I_α^j, $\alpha = x, y, z$ are the spin operators of the j'th nucleus, θ is the tilt angle of the quadrupolar axis away from z and $B_{\rm Q}$ is the quadrupolar interaction strength. The low-energy excitations of the system are obtained through a Schrieffer-Wolff transformation perturbative in $B_{\rm Q}/\omega_{\rm Z}^{\rm n}$, which replaces $H_{\rm Q}$ by $H_{\rm Q}^0 + V_{\rm Q}'$. $H_{\rm Q}^0$ commutes with I_z^j and $V_{\rm Q}' = S_z[\mathcal{A}_1(\Phi_1^+ + \Phi_1^-) + \mathcal{A}_2(\Phi_2^+ + \Phi_2^-)]$ is a non-collinear hyperfine interaction [19, 25]. Here, Φ_ζ^+ ($\zeta = 1, 2$) denotes the nuclear spin wave operators

$$\Phi_1^+ = \sum_j a_j[I_+^j I_z^j + I_z^j I_+^j], \;\; \Phi_2^+ = \sum_j a_j (I_+^j)^2,$$

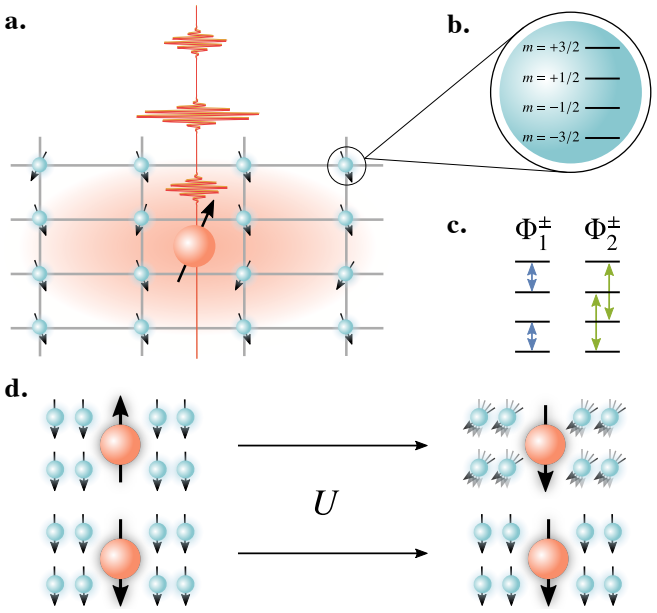

FIG. 1. **a.** System schematic comprising a pulse-driven electron coupled to a mesoscopic bath of nuclear spins **b.** Structure of the high-spin ($I > 1/2$) nuclei, here shown for $I = 3/2$. **c.** Spin transitions between states in b. generated by the non-collinear processes $\Phi_1^{\pm}$ and $\Phi_2^{\pm}$ **d.** In the memory write-in process, the stimulated electron–nuclear interaction flips the electron and generates a nuclear spin wave conditionally on the electron spin, thereby transferring the electron state to the nuclear ensemble. Here, the time-evolution operator, $U = e^{-i\mathcal{H}_I \pi/(2g_\zeta)}$, corresponds to the evolution in Eq. (2) at time $t = \pi/(2g_\zeta)$.

with $\Phi_\zeta^- = (\Phi_\zeta^+)^\dagger$; thus $\Phi_\zeta^\pm$ changes the net nuclear spin by $\pm\zeta$ as shown in Fig. 1b-c. The overall strength of the interaction is given by $\mathcal{A}_1 = \frac{1}{2}\sum_j A^j B_Q \sin 2\theta/\omega_Z^n$ and $\mathcal{A}_2 = \frac{1}{2}\sum_j A^j B_Q \sin^2\theta/\omega_Z^n$, and $a_j = A^j/\sum_{j'} A^{j'}$ are the normalised hyperfine coefficients. A quadrupolar coupling strength of $B_Q = 1.5$ MHz, which is typical of naturally occuring strain [26] or which can be engineered in situ [27, 28], will be considered here.

A nuclear spin transition corresponding to the action of $\Phi_\zeta^\pm$ costs an energy of $\zeta\omega_Z^n$, which in a strong magnetic field is considerably larger than the transition matrix elements of V_Q'. Consequently, these processes are far off-resonance in equilibrium. To switch the interaction on, we follow Ref. [21] and consider the action of a pulse sequence on the electron spin, driving it with a set of short S_x and S_y pulses separated by a time interval, $\tau/4$. By setting $\tau = \ell\pi/(\zeta\omega_Z^n)$, where ℓ is an odd integer, the coupling between the electron and the Φ_ζ-mode is resonantly enhanced, and the system will evolve under an effective flip-flop Hamiltonian [25]

$$\mathcal{H}_I = \mathcal{A}_\zeta'(\Phi_\zeta^+ S_- + \Phi_\zeta^- S_+), \tag{1}$$

where $S_\pm = S_x \pm iS_y$ are the electron spin-flip operators and $\mathcal{A}_\zeta'$ is a rescaled coupling rate taking its maximal value for $\ell = 3$, where $\mathcal{A}_\zeta' = (2+\sqrt{2})/(3\pi)\mathcal{A}_\zeta$. When the nuclei are initialised in a fully polarised state, this Hamiltonian will create a nuclear spin wave and flip the electron spin conditionally on the electron spin state (see Fig. 1d), thus forming the basis of information transfer between the electron and nuclear ensemble. While realistic quantum dots comprise nuclei of several species, we show [25] that under a magnetic field sufficiently strong to energetically resolve each species, the pulse sequence can couple the electron to a single species.

To see how this protocol turns nuclear spins into a quantum memory, we first consider a perfectly polarised nuclear bath (see Fig. 2a). We write this nuclear state as $|\mathbf{0}\rangle = |-I,\cdots,-I\rangle$, and take the electron to be initialised in the state $|\phi\rangle = \alpha|\uparrow\rangle + \beta|\downarrow\rangle$, which we want to transfer to the nuclei. Because the nuclei are initialised in the ground state, no downwards transition are possible and $\Phi_\zeta^-|\mathbf{0}\rangle = 0$. The excited nuclear state $|\mathbf{1}\rangle \propto \Phi_\zeta^+|\mathbf{0}\rangle$ is a distributed superposition of nuclear excitations (indicated by blue dots in Fig. 2a), $\sum_j a_j|-I,\cdots,(-I+\zeta)_j,\cdots,-I\rangle$. Crucially, when de-exciting the spin wave, the only downwards nuclear transitions available are those that were excited from the ground state, and thus $\Phi_\zeta^-|\mathbf{1}\rangle \propto |\mathbf{0}\rangle$. Due to these properties, the system evolves within a three dimensional subspace as

$$|\psi(t)\rangle = \alpha\left[\cos g_\zeta t\,|\uparrow\rangle\otimes|\mathbf{0}\rangle - i\sin g_\zeta t\,|\downarrow\rangle\otimes|\mathbf{1}\rangle\right] + \beta|\downarrow\rangle\otimes|\mathbf{0}\rangle, \tag{2}$$

$g_\zeta = F_\zeta\mathcal{A}_\zeta'\sqrt{\sum_j a_j^2}$ (scaling as $\sqrt{N}$) is a collectively enhanced non-collinear coupling rate, where $F_1 = (1-2I)\sqrt{2I}$, $F_2 = 2\sqrt{I(2I-1)}$. At time $t = \pi/(2g_\zeta)$ the electron–nuclear wavefunction separates, $|\psi(\pi/2g_\zeta)\rangle = |\downarrow\rangle\otimes(-i\alpha|\mathbf{0}\rangle + \beta|\mathbf{1}\rangle)$, and the electron state is identically transferred to the collective state of the nuclei to be stored.

Operation at partial nuclear polarisation — A realistic implementation will initialise the nuclei in a partially polarised state [29], $|M\rangle = |m_1,\cdots,m_N\rangle$, such that there is a small number of lower energy states to scatter into, and thus $\Phi_\zeta^-|M\rangle \neq 0$ (see Fig. 2b). Accordingly, the downwards transition $|M\rangle \to \Phi_\zeta^-|M\rangle$ is no longer forbidden as in the perfectly polarised case, but will take place with a rate, $\mathcal{G}_-$, which is slower than the upwards coupling rate, $\mathcal{G}_+$. Similarly, the downwards transition Φ_ζ^- from the excited state $\Phi_\zeta^+|M\rangle$ does not lead back to $|M\rangle$ but mixes with other states generated by de-excitation of the initially unpolarised nuclei. This leads to dephasing of the spin wave mode serving as quantum memory. Nonetheless, the asymmetry of the coupling rates ($\mathcal{G}_+ > \mathcal{G}_-$) makes it possible to operate the quantum memory at finite polarisations.

To calculate the electron–nuclear dynamics during the pulse sequence, we have developed a numerically exact technique that maps the nuclear many-body state onto two one-dimensional chains of states, $\hat{\mathcal{S}}_\pm = \{|\hat{M}_\pm^{(k)}\rangle | k = 0,\cdots,N\}$. Here, the initial state $|\hat{M}_+^{(0)}\rangle = |\hat{M}_-^{(0)}\rangle = |M\rangle$ appears as the first link in both chains. The set $\hat{\mathcal{S}}_+$ ($\hat{\mathcal{S}}_-$) represents the set of states tied with the evolution of a positive (negative) spin wave. The coupling structure of $\mathcal{H}_I$, taking the electron spin

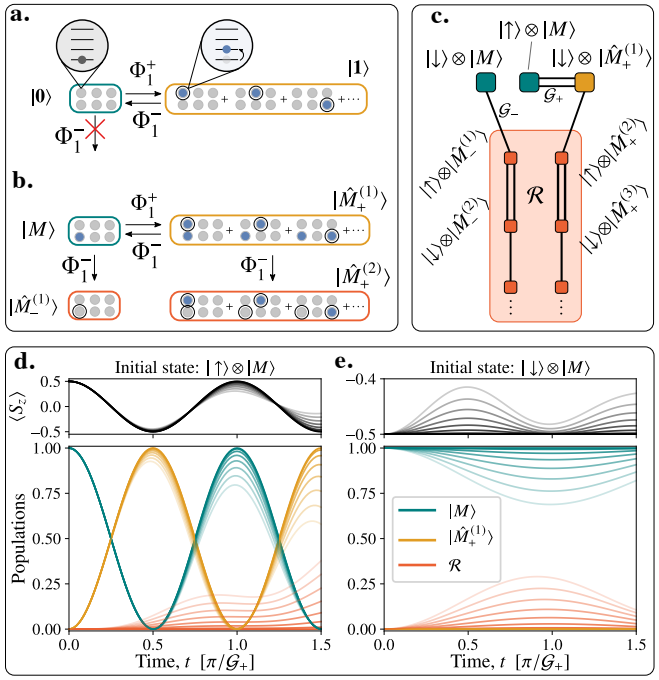

FIG. 2. **a.** Collective spin wave excitation starting from a fully polarised state, where all nuclei are in the ground state (grey dots). The black circles emphasise the nuclei that have exchanged energy with the electron. The spin wave contains a single nuclear excitation (blue dots) distributed among all of the nuclei in a superposition. **b.** Spin wave excitation from finitely polarised nuclear product state, $|M\rangle$, to target state, $|\hat{M}_+^{(1)}\rangle$, where initially excited nuclei allow leakage transitions respectively to orthogonal states $|\hat{M}_-^{(1)}\rangle$ and $|\hat{M}_+^{(2)}\rangle$. **c.** Coupling structure in 1D mapping of nuclear state space. The initial state is a superposition of the two green states, and interactions couple these initial states to a 1D structure of states. Double lines signify the fast coupling rate $\mathcal{G}_+$, and single lines the slow rate, $\mathcal{G}_-$. For a fully polarised ensemble $\mathcal{G}_- = 0$ and the three upper states remain isolated; at finite polarisation, this subspace is coupled to the residual chain of states, $\mathcal{R}$. **d.-e.** Dynamics for initialisation in electron states $|\uparrow\rangle$ and $|\downarrow\rangle$, respectively. Solid lines signify the fully polarised case, where $\mathcal{G}_- = 0$. Lines with decreased opacity signify decreased polarisation and thus increased $\mathcal{G}_-$-rate, with the maximal value $\mathcal{G}_-/\mathcal{G}_+ = 0.3$. Line colors correspond to states in panel c.

into account as well, is illustrated in Fig. 2c, where a coupling rate of $\mathcal{G}_+$ between two neighbouring states is depicted with a double line and $\mathcal{G}_-$ with a single line. In the Supplemental Material we derive the form of the basis sets $\hat{\mathcal{S}}_\pm$ and show that only neighbouring nuclear states are coupled by the spin wave operators entering $\mathcal{H}_I$,

$$\begin{aligned}\langle \hat{M}_+^{(2n\pm1)}|\Phi_\zeta^+|\hat{M}_+^{(2n)}\rangle &= \langle \hat{M}_-^{(2n)}|\Phi_\zeta^+|\hat{M}_-^{(2n\mp1)}\rangle = \mathcal{G}_\pm/\mathcal{A}'_\zeta \\ \langle \hat{M}_+^{(2n)}|\Phi_\zeta^-|\hat{M}_+^{(2n\pm1)}\rangle &= \langle \hat{M}_-^{(2n\mp1)}|\Phi_\zeta^-|\hat{M}_-^{(2n)}\rangle = \mathcal{G}_\pm/\mathcal{A}'_\zeta.\end{aligned} \tag{3}$$

The asymmetry in rates is parametrised by a leakage factor, $\mathcal{G}_-/\mathcal{G}_+$, which indicates the extent to which the nuclear phase space is explored in the evolution. In the fully polarised case, where the initial state is $|M\rangle = |\mathbf{0}\rangle$ (and $|\hat{M}_+^{(1)}\rangle = |\mathbf{1}\rangle$), we find $\mathcal{G}_+ = g_\zeta$, $\mathcal{G}_- = 0$ (no leakage), meaning that the three states $|\uparrow\rangle\otimes|M\rangle, |\downarrow\rangle\otimes|\hat{M}_+^{(1)}\rangle, |\downarrow\rangle\otimes|M\rangle$ are completely decoupled from the residual part of the two chains (which in Fig. 2c is signified by $\mathcal{R}$), recovering the ideal state transfer dynamics of Eq. (2). For finite initial nuclear polarisation, we generally have $\mathcal{G}_+ < g_\zeta$ and $\mathcal{G}_- > 0$ (finite leakage), and thus the three states couple to the residual chains, $\mathcal{R}$. Figs. 2d-e show the electron and nuclear dynamics as the leakage factor $\mathcal{G}_-/\mathcal{G}_+$ is gradually changed from the ideal case of 0 (solid lines) to 30% in linear steps (decreasing opacity). As $\mathcal{G}_-$ is increased, the system is more rapidly delocalised along the chain, leading to uncontrollable electron–nuclear correlations that are seen as damped oscillations in the nuclear and electronic populations. When calculating the dynamics, it is necessary to truncate the nuclear chains of states to a certain k-index, k^*. As long as the occupation of the states $|\hat{M}_\pm^{(k^*)}\rangle$ is sufficiently small, the truncation remains a valid approximation. The necessary value of k^* needed for convergence depends on the evolution time and the leakage factor $\mathcal{G}_-/\mathcal{G}_+$, which together determine how far into $\mathcal{R}$ the state will diffuse.

Fig. 3a shows the ratio $\mathcal{G}_-/\mathcal{G}_+$ as a function of nuclear polarisation, averaged over the nuclear initial state distribution, $p(M)$. This distribution is taken as thermal at the polarisation-dependent temperature T, i.e. $p(M) \sim \prod_j \exp[-m_j\omega_Z^{\mathrm{n}}/(k_{\mathrm{B}}T)]$, where k_{B} is the Boltzmann constant [25], for $I = 3/2$ and $N \simeq 5\times10^4$ (see Fig. 3a). The relative ensemble standard deviations (not shown) are negligible, $\sim 10^{-3}$. An important conclusion drawn from Fig. 3a is that the $\zeta = 2$ mode is more robust towards imperfect polarisation, owing to the different dependence of the leakage factor $\mathcal{G}_-/\mathcal{G}_+$ on polarisation for $\zeta = 1$ and $\zeta = 2$. The Φ_2^--transition becomes dark when the levels $m = +3/2$, $m = +1/2$ are depleted, whereas for Φ_1^-, the level $m = -1/2$ needs to be depleted for this to happen. Indeed, the lower levels of a single spin manifold (Fig. 1b) will be populated first, as the polarisation is decreased, thus enabling the Φ_1^- transition before the Φ_2^- transition.

Fig. 3b shows the calculated values of $\mathcal{G}_+$ as a function of nuclear Zeeman splitting, where the lines indicate a polarisation of 50% and the shaded area shows the variation as the polarisation is sweeped from unity (maximum values) to 0 (minimum values). The coupling rate $\mathcal{G}_+$ is proportional to $\sin(2\theta)$ for the $\zeta = 1$ mode and to $\sin^2\theta$ for $\zeta = 2$. These angular prefactors have been assumed to be unity to maximise the rates shown in Fig. 3b, which can be converted to rates for any quadrupolar angle by multiplying them with these prefactors.

State transfer fidelity — The state transfer fidelity is defined as the overlap between the initial electron state and the electron state after a full write–read cycle. We initialise the system in the state $|\psi(0)\rangle = |\phi\rangle\otimes|M\rangle$ and let it evolve under the pulse sequence for a time t_1 to write the electron state into the nuclei, thus generating the state $|\psi(t_1)\rangle$. After this, we trace out the electron to obtain the reduced nuclear state $\rho_{\mathrm{n}}(t_1) = \mathrm{Tr}_{\mathrm{e}}[\,|\psi(t_1)\rangle\langle\psi(t_1)|]$. To read the nuclear state back into the electron spin, we re-initialise the density operator in the state $\rho(t_1;0) = |\downarrow\rangle\langle\downarrow|\otimes\rho_n(t_1)$ and let the system evolve under the pulse sequence for a time t_2, where the total density

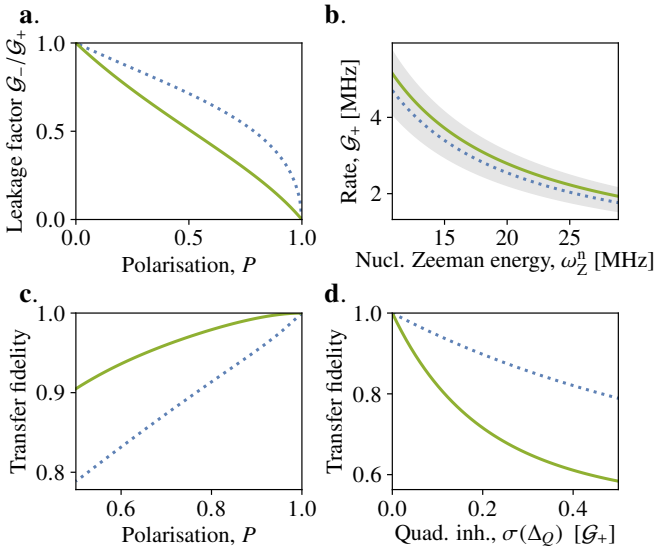

FIG. 3. **a.** Leakage factor as ratio of coupling rates, $\mathcal{G}_-/\mathcal{G}_+$ as a function of nuclear polarisation. Green solid (blue dotted) lines denote $\zeta = 2$ ($\zeta = 1$). **b.** Coupling rate $\mathcal{G}_+$ for $\zeta = 1$ (blue dotted) and $\zeta = 2$ (green solid) at $P = 0.5$ for varying nuclear Zeeman splitting. The shaded area corresponds to the range of values from $P = 0$ to $P = 1$. **c.** Transfer fidelity of total write-in and read-out cycle as a function of polarisation. **d.** Transfer fidelity of total write-in and read-out cycle at full polarisation ($P = 1$) as a function of inhomogeneity in quadrupolar energy shift.

operator is $\rho(t_1;t_2)$. We then evaluate the overlap of the electron spin state (tracing out the nuclei) with respect to the input state to assess the fidelity, $\mathcal{F}(t_1,t_2) = \mathrm{Tr}_n[\langle\phi'|\rho(t_1;t_2)|\phi'\rangle]$, where $|\phi'\rangle = \alpha|\uparrow\rangle - \beta|\downarrow\rangle$. The fidelity is then averaged over the six states $(\alpha,\beta) = (1,0),(0,1),\frac{1}{\sqrt{2}}(1,\pm1),\frac{1}{\sqrt{2}}(1,\pm i)$, and there is a unique combination of write-in (t_1) and read-out (t_2) times, found numerically, that maximise this fidelity. In the fully polarised case, the optimal t_1 and t_2 are simply $\pi/(2\mathcal{G}_+)$, but as the polarisation is decreased, coupling to $\mathcal{R}$ necessitates slightly (< 20%) longer transfer times. The time-optimised fidelity is presented in Fig. 3c, which confirms that it follows the polarisation dependence of the leakage factor, $\mathcal{G}_-/\mathcal{G}_+$, and accordingly that the fidelity is generally higher for the $\zeta = 2$ mode if the polarisation is finite. In particular, for $\zeta = 2$, the fidelity remains above 90% throughout the polarisation range $50-100\%$.

Adjusting to quadrupolar energy shifts — The I_z^j-commuting contribution to the quadrupolar Hamiltonian can be written as $H_Q^0 = \sum_j \Delta_Q (I_z^j)^2$, with $\Delta_Q = B_Q(\cos^2\theta - \frac{1}{2}\sin^2\theta)$. In general, Δ_Q varies over the ensemble, and the individual spin components in the spin wave $|\mathbf{1}\rangle$ evolve with a phase factor $e^{-i\zeta^2\Delta_Q^j t}$, building up a relative phase among the components on a time scale set by the ensemble variation of Δ_Q^j, denoted by $\sigma(\Delta_Q)$. As a result, $|\mathbf{1}\rangle$ rotates into a dark subspace, $\{|1_p\rangle\}$, such that $\Phi_-|1_p\rangle = 0$ with a rate of $\gamma = \zeta^2\sigma(\Delta_Q)$ [25]. In Fig. 3d, we show how the transfer fidelity at full nuclear polarisation depends on this inhomogeneity. As indicated, the energy scale of the inhomogeneity, $\sigma(\Delta_Q)$ must be compared to the coupling rate, $\mathcal{G}_+$, to assess its impact. Thus, with a realistic value of $\mathcal{G}_+$ in the MHz range, a quadrupolar inhomogeneity below ~ 100 kHz, achievable e.g. through lattice-matched epitaxial quantum dot growth [29], does not degrade the transfer fidelity appreciably. Importantly, decoherence due to rotation into the dark subspace is only of concern during the transfer process: after the state has been transferred, the collective phase of the nuclear excitation can be refocused through an NMR pulse sequence operating on the $\{m = -I, m = -I + \zeta\}$ subspace [17, 25, 30]. In the case of a non-zero mean value of Δ_Q, the $m = -I$ to $m = -I + \zeta$ transition is shifted by $\delta = (\zeta^2 - 2I\zeta)\Delta_Q$. The memory transfer is then simply effectuated by setting the pulse time delay to $\tau = \ell\pi/(\zeta\omega_Z^n + \delta)$.

During storage, we expect the dominant nuclear dephasing mechanism that determines the coherence time of the memory to be the electron–mediated nuclear dipole-dipole interaction, which scales inversely with the electron Zeeman splitting [18]. In the presence of this dephasing mechanism, the coherence time of the nuclear memory is tens of microseconds. If, however, the electron is removed from the quantum dot after its state is transferred to the nuclei, the only dephasing mechanism is the intrinsic neighbour dipole-dipole interaction, and the coherence time can be well into the millisecond regime [16, 17, 24]. Importantly, the nuclei should be polarised as to increase the electron Zeeman splitting. This way, nuclear polarisation leads not only to increased fidelity in the transfer process, but also to a prolonged storage time.

Conclusion — We have proposed a scheme for collective quantum memory, which can reach transfer fidelities for a full read-write cycle as high as 90% with a modest nuclear polarisation of 50% for realistic experimental parameters. In addition, the theoretical and experimental techniques we have presented open new possibilities for further exploration and manipulation of the collective nuclear degrees of freedom, for example the generation of nuclear cat states, squeezed states and condensates.

Acknowledgements — We thank E. Chekhovich for helpful discussions. This work was supported by the ERC PHOENICS grant (617985), the EPSRC Quantum Technology Hub NQIT (EP/M013243/1) and the Royal Society (RGF/EA/181068). D.A.G. acknowledges support from St John's College Title A Fellowship. E.V.D. and J.M. acknowledge funding from the Danish Council for Independent Research (Grant No. DFF-4181-00416). C.L.G. acknowledges support from a Royal Society Dorothy Hodgkin Fellowship.

* Electronic address: cl538@cam.ac.uk

[1] H.-J. Briegel, W. Dür, J. I. Cirac, and P. Zoller, Physical Review Letters **81**, 5932 (1998).
[2] H. J. Kimble, Nature **453**, 1023 (2008).
[3] A. E. Kozhekin, K. Mølmer, and E. Polzik, Physical Review A **62**, 033809 (2000).

[4] B. Julsgaard, J. Sherson, J. I. Cirac, J. Fiurášek, and E. S. Polzik, Nature **432**, 482 (2004).

[5] K. S. Choi, A. Goban, S. B. Papp, S. J. Van Enk, and H. J. Kimble, Nature **468**, 412 (2010).

[6] R. Zhao, Y. O. Dudin, S. D. Jenkins, C. J. Campbell, D. N. Matsukevich, T. A. B. Kennedy, and A. Kuzmich, Nature Physics **5**, 100 (2009).

[7] M. P. Hedges, J. J. Longdell, Y. Li, and M. J. Sellars, Nature **465**, 1052 (2010).

[8] W. Tittel, M. Afzelius, T. Chaneliere, R. L. Cone, S. Kröll, S. A. Moiseev, and M. Sellars, Laser & Photonics Reviews **4**, 244 (2010).

[9] D. Kielpinski, V. Meyer, M. A. Rowe, C. A. Sackett, W. M. Itano, C. Monroe, and D. J. Wineland, Science **291**, 1013 (2001).

[10] C. Langer, R. Ozeri, J. D. Jost, J. Chiaverini, B. DeMarco, A. Ben-Kish, R. B. Blakestad, J. Britton, D. B. Hume, W. M. Itano, *et al.*, Physical Review Letters **95**, 060502 (2005).

[11] M. V. G. Dutt, L. Childress, L. Jiang, E. Togan, J. Maze, F. Jelezko, A. Zibrov, P. R. Hemmer, and M. D. Lukin, Science **316**, 1312 (2007).

[12] G. D. Fuchs, G. Burkard, P. V. Klimov, and D. D. Awschalom, Nature Physics **7**, 789 (2011).

[13] T. H. Taminiau, J. Cramer, T. van der Sar, V. V. Dobrovitski, and R. Hanson, Nature Nanotechnology **9**, 171 (2014).

[14] J. M. Taylor, C. M. Marcus, and M. D. Lukin, Physical Review Letters **90**, 206803 (2003).

[15] J. M. Taylor, A. Imamoglu, and M. D. Lukin, Physical Review Letters **91**, 246802 (2003).

[16] Z. Kurucz, M. W. Sørensen, J. M. Taylor, M. D. Lukin, and M. Fleischhauer, Physical Review Letters **103**, 010502 (2009).

[17] E. A. Chekhovich, M. Hopkinson, M. S. Skolnick, and A. I. Tartakovskii, Nature Communications **6**, 6348 (2015).

[18] G. Wüst, M. Munsch, F. Maier, A. V. Kuhlmann, A. Ludwig, A. D. Wieck, D. Loss, M. Poggio, and R. J. Warburton, Nature Nanotechnology **11**, 885 (2016).

[19] D. A. Gangloff, G. Ethier-Majcher, C. Lang, E. V. Denning, J. H. Bodey, D. Jackson, E. Clarke, M. Hugues, C. Le Gall, and M. Atatüre, Science **364**, 62 (2019).

[20] A. Högele, M. Kroner, C. Latta, M. Claassen, I. Carusotto, C. Bulutay, and A. Imamoglu, Physical Review Letters **108**, 197403 (2012).

[21] I. Schwartz, J. Scheuer, B. Tratzmiller, S. Müller, Q. Chen, I. Dhand, Z.-Y. Wang, C. Müller, B. Naydenov, F. Jelezko, *et al.*, Science Advances **4**, eaat8978 (2018).

[22] J. H. Bodey, R. Stockill, E. V. Denning, D. A. Gangloff, G. Ethier-Majcher, D. M. Jackson, E. Clarke, M. Hugues, C. Le Gall, and M. Atatüre, arXiv preprint, arXiv:1906.00427 (2019).

[23] W. Yao, R.-B. Liu, and L. J. Sham, Physical Review B **74**, 195301 (2006).

[24] C. Deng and X. Hu, IEEE Transactions on Nanotechnology **4**, 35 (2005).

[25] See Supplemental Material [URL] for detailed derivations and descriptions of the results, which includes Refs. [31–34].

[26] C. Bulutay, Physical Review B **85**, 115313 (2012).

[27] X. Yuan, F. Weyhausen-Brinkmann, J. Martín-Sánchez, G. Piredda, V. Křápek, Y. Huo, H. Huang, C. Schimpf, O. G. Schmidt, J. Edlinger, *et al.*, Nature Communications **9**, 3058 (2018).

[28] K. Flisinski, I. Y. Gerlovin, I. V. Ignatiev, M. Y. Petrov, S. Y. Verbin, D. R. Yakovlev, D. Reuter, A. D. Wieck, and M. Bayer, Physical Review B **82**, 081308 (2010).

[29] E. A. Chekhovich, A. Ulhaq, E. Zallo, F. Ding, O. G. Schmidt, and M. S. Skolnick, Nature materials **16**, 982 (2017).

[30] B. Albrecht, P. Farrera, G. Heinze, M. Cristiani, and H. de Riedmatten, Physical Review Letters **115**, 160501 (2015).

[31] B. Urbaszek, X. Marie, T. Amand, O. Krebs, P. Voisin, P. Maletinsky, A. Högele, and A. Imamoglu, Reviews of Modern Physics **85**, 79 (2013).

[32] Y. H. Huo, B. J. Witek, S. Kumar, J. R. Cardenas, J. X. Zhang, N. Akopian, R. Singh, E. Zallo, R. Grifone, D. Kriegner, *et al.*, Nature Physics **10**, 46 (2014).

[33] J. R. Johansson, P. D. Nation, and F. Nori, Computer Physics Communications **184**, 1234 (2013).

[34] E. A. Chekhovich, I. M. Griffiths, M. S. Skolnick, H. Huang, S. F. C. da Silva, X. Yuan, and A. Rastelli, Physical Review B **97**, 235311 (2018).